3.3 Bundle Solution

Summary: The method of self-calibration has proved to be one of the most powerful calibration techniques. If used in the context of a general bundle solution it provides for object space coordinates or object features, camera exterior and interior orientation parameters, and models other systematic errors as well. Therefore, because of its flexibility, it may be used in stereo, multi-frame systems, egomotion computations, etc. This chapter gives a brief introduction into the principle of self-calibration, emphasizes some of the problems which are associated with it, and demonstrates with practical data to what extent geometry and network design will influence the determinability of the self-calibration parameters. Finally, a system test will show the high accuracy performance of self-calibrating CCD-camera systems.

3.3.1 Introduction

Since photogrammetry has always been concerned with precise measurements using images, the accurate calibration of the sensors used has been, and still is, of major concern. In the case of a single frame camera sensor (photographic or opto-electronic) the underlying geometrical model for processing is that of perspective projection and the associated procedure for the adjustment of the image coordinate measurements and the estimation of the derived parameters is the "bundle method". The fundamental projection parameters are the image coordinates of the principal point and the camera constant. They define the interior orientation of a CCD-frame. According to a widespread definition some authors also include the lens distortion (very often only the radial part) into the set of parameters for interior orientation. These parameters may be systematically distorted. However, there are a great number of additional error sources which may lead to a deformation of the imaging bundle of rays and thus contribute to the overall systematic error budget. Among the most prominent in photographic systems are film and emulsion distortion, unflatness of the imaging plane, false fiducial mark coordinates, effects of image motion, and atmospheric refraction. In CCD-camera based systems not all of those are relevant, but one has to consider a number of additional distortion sources as identified by *Gruen* [1] and investigated by *Beyer* [2] and [3].

We define now "system calibration" as a technique which reduces the original image data such that it is most compatible with the chosen parameters of perspective projection. This may include an estimation and correction of these latter parameters themselves.

In Section 3.3.2 the method of self-calibration, a technique for system calibration which was introduced into photogrammetry twenty years ago, is briefly described.

Self-calibration is a standard procedure in aerial photogrammetry. Under operational conditions it leads to accuracy improvements of up to a factor 3. It is of particular value in CCD-based close-range systems since the cameras and framegrabbers used are commonly poorly calibrated or the calibration parameters might significantly change over time (camera constant and lens distortion through focussing, principal point through warm-up effects, etc.). Accuracy improvement factors of up to 10 were observed in controlled test projects by *Gruen* et al. [4] and by *Beyer* [2, 3]. Since self-calibration adds new parameters to the linearized system of bundle adjustment there is a certain danger of overparameterization, which could lead to ill-conditioning or even singularity of the normal equations of least squares adjustment.

Section 3.3.3 demonstrates how geometry and network design influence the determinability of the self-calibration parameters.

Section 3.3.4 shows the potential of this technique in a controlled test and proves the high accuracy performance of CCD-camera based systems.

3.3.2 The concept of self-calibration

If single-frame camera data is processed, for instance in CCD-camera applications, the geometric sensor model is that of perspective projection, leading to the so-called "bundle method". This bundle method is considered the most flexible, general and accurate sensor model. Long before it became a standard procedure in aerial photogrammetry it was used in a variety of close-range applications. Since, for the method of self-calibration presented here, the bundle method is the underlying estimation model the latter will be very briefly addressed in the following (there exists an abundance of publications on this subject in the photogrammetric literature, e.g. [5, 6, 7, 8, 9].

3.3.2.1 The bundle method

The basis of the bundle method is the collinearity condition (compare also Figure 1)

$$\begin{bmatrix} X \\ Y \\ Z \end{bmatrix}_i = \lambda_{ij} \boldsymbol{R}_j \begin{bmatrix} x_{ij} - x_{0j} \\ y_{ij} - y_{0j} \\ 0 - c_j \end{bmatrix} + \begin{bmatrix} X_0 \\ Y_0 \\ Z_0 \end{bmatrix}_j \tag{1}$$

with

X_i, Y_i, Z_i	Object space coordinates of object point (P_i)
X_{0j}, Y_{0j}, Z_{0j} ...	Object space coordinates of perspective center (O_j)
$x_{ij}, y_{ij}, 0$	Measured image coordinates of point (P'_{ij})
$x_{0j}, y_{0j},$	Image space coordinates of principal point (H'_j)
c_j	Camera constant of CCD-frame j
$\boldsymbol{R_j}$	Rotation matrix (orthogonal) between image and object space coordinate systems
λ_{ij}	Scale factor for imaging ray

$i = 1, \ldots,$ nop (nop = number of object points)
$j = 1, \ldots,$ nof (nof = number of CCD frames)

In (1) the interior orientation of a CCD-frame j is defined by the parameters x_{0j}, y_{0j}, c_j while the parameters X_{0j}, Y_{0j}, Z_{0j}, $\boldsymbol{R_j}(\varphi_j, \omega_j, \kappa_j)$define the exterior orientation. Here $\varphi_j, \omega_j, \kappa_j$ are the three rotation angles which build up the rotation matrix $\boldsymbol{R}_j$. The three components in (1) are reduced to two by cancelling out the scale factor λ_{ij}, and then rearranged according to

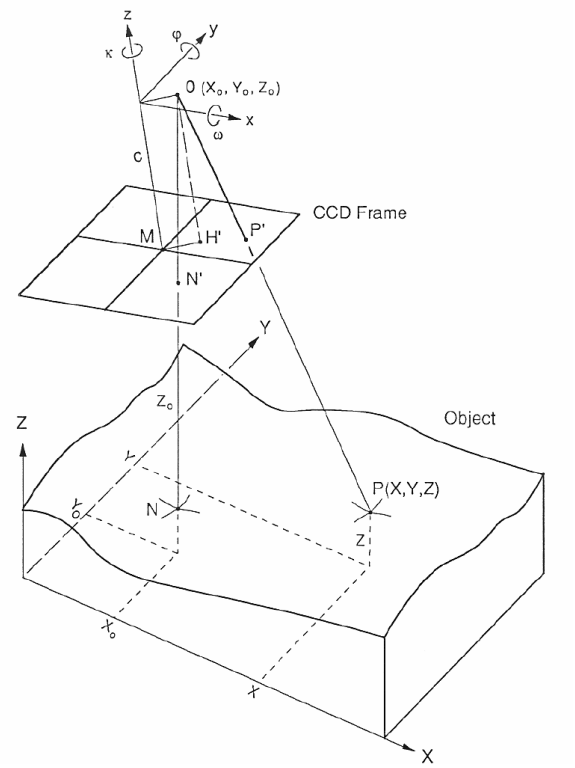

Figure 1: : Sensor model of the bundle method

$$
\begin{aligned}
x_{ij} &= -c_j f_{ij}^x + x_{0j} = -c_j \frac{r_{11j}(X_i - X_{0j}) + r_{21j}(Y_i - Y_{0j}) + r_{31j}(Z_i - Z_{0j})}{r_{13j}(X_i - X_{0j}) + r_{23j}(Y_i - Y_{0j}) + r_{33j}(Z_i - Z_{0j})} + x_{0j} \\
y_{ij} &= -c_j f_{ij}^y + y_{0j} = -c_j \frac{r_{12j}(X_i - X_{0j}) + r_{22j}(Y_i - Y_{0j}) + r_{32j}(Z_i - Z_{0j})}{r_{13j}(X_i - X_{0j}) + r_{23j}(Y_i - Y_{0j}) + r_{33j}(Z_i - Z_{0j})} + y_{0j}
\end{aligned}
\tag{2}
$$

$r_{11j} \ldots r_{33j}$ are the elements of $\vec{R}_j$.

Since (2) provide for a general sensor model they accommodate easily the specific cases which are often treated in computer vision, e.g. stereo, egomotion, etc.. Depending on the parameters which are considered either known a priori or treated as unknowns these equations may result in the following cases, which are also listed in Table 1 (x_{ij}, y_{ij} are always regarded as observed quantities):

(a) General bundle method: All parameters on the right hand side of (2) are unknown (interior orientation, exterior orientation, object point coordinates).

(b) Bundle method for "metric camera" systems: x_{0j}, y_{0j}, c_j (interior orientation) are given, all others unknown.

(c) Spatial resection:

Table 1: Photogrammetric orientation and point positioning procedures as special cases of the general bundle method

Procedure	Given Parameters	Unknown Parameters
General bundle	-	$(X,Y,Z)_i; IO_j; EO_j$
Metric camera bundle	IO_j	$(X,Y,Z)_i; EO_j$
Spatial resection (a)	$IO_j; (X,Y,Z)_i$	EO_j
(b)	$(X,Y,Z)_i$	$IO_j; EO_j$
Spatial Intersection (Stereo or multiframe)	$IO_j; EO_j$	$(X,Y,Z)_i$

IO ... Interior orientation, EO... Exterior orientation

(ca) Interior orientation and object point coordinates (X_i, Y_i, Z_i) are given, the exterior orientation has to be determined.

(cb) Only object point coordinates are given, the interior and exterior orientation have to be determined.

(d) Spatial intersection: The interior and exterior orientation are given, the object point coordinates have to be determined. This includes the stereo as well as the multiframe approaches.

Any combination of procedures is possible within the general bundle concept. Also incomplete parameter sets of exterior/interior orientation and object points can be treated.

3.3.2.2 Least squares estimation

Equations (2) are considered observation equations functionally relating the observations x_{ij}, y_{ij} to the parameters of the right hand side according to

$$\boldsymbol{l} = f(\boldsymbol{x}) \; . \tag{3}$$

For the estimation of $\boldsymbol{x}$ the Gauss-Markov model of least squares is used. After linearization of (3) and the introduction of a true error vector $\boldsymbol{e}$ we obtain

$$\boldsymbol{l} - \boldsymbol{e} = \boldsymbol{A}\boldsymbol{x} \; . \tag{4}$$

The design matrix $\boldsymbol{A}$ is a n x u matrix (n ..... number of observations,u .... number of unknown parameters), with $n \geq u$ and, in general, rank $(\boldsymbol{A})= u$.

With the assumed expectation $E(\boldsymbol{e})= \boldsymbol{0}$ and the dispersion operator D we get

$$\begin{aligned} E(\boldsymbol{l}) &= \boldsymbol{A}\boldsymbol{x} \; , \\ D(\boldsymbol{l}) &= \boldsymbol{C}_{ll} = \sigma_0^2 \boldsymbol{P}^{-1}, \\ D(\boldsymbol{e}) &= \boldsymbol{C}_{ee} = \boldsymbol{C}_{ll} \; . \end{aligned} \tag{5}$$

$\boldsymbol{P}$ is the "weight coefficient" matrix of $\boldsymbol{l}$ and $\boldsymbol{C}$ stands for covariance operator, σ_0^2 is the variance factor.

The estimation of $\boldsymbol{x}$ and σ_0^2 is usually (not exclusively) attempted as unbiased, minimum variance estimation, performed by means of least squares, and results in:

$$\begin{aligned} \hat{\boldsymbol{x}} &= \left(\boldsymbol{A}^T\boldsymbol{P}\boldsymbol{A}\right)^{-1}\boldsymbol{A}^T\boldsymbol{P}\boldsymbol{l}\,, \\ \boldsymbol{v} &= \boldsymbol{A}\hat{\boldsymbol{x}}-\boldsymbol{l}\,, \\ \hat{\sigma}_0^2 &= \frac{\boldsymbol{v}^T\boldsymbol{P}\boldsymbol{v}}{r},\quad r=n-u\,. \end{aligned} \tag{6}$$

$\boldsymbol{v}$... Residuals of least squares.

The structure of $\boldsymbol{A}$ is determined by the procedure applied (compare Table 1), it reflects the overall network design and thus also the geometrical and numerical stability of the arrangement.

For $\boldsymbol{A}^T\boldsymbol{P}\boldsymbol{A}$ to be uniquely invertible, as required in (6), the network needs an external "datum", that is, the seven parameters of a spatial similarity transformation of the network need to be fixed. This is usually achieved either by introducing control points with seven fixed coordinate values, or by fixing seven appropriate elements of the exterior orientations of two frames.The precision of the parameter vector $\boldsymbol{x}$ is controlled by its covariance matrix $\boldsymbol{C}_{xx} = \hat{\sigma}_0^2\left(\boldsymbol{A}^T\boldsymbol{P}\boldsymbol{A}\right)^{-1}$.

3.3.2.3 Systematic error compensation by self-calibration

For systematic error compensation a number of methods have evolved over the years, among which the following are the most prominent:

A priori:
- Data reduction using physical models
- Laboratory calibration
- Réseau corrections
- Testfield calibration under project conditions

A posteriori:
- Post-treatment of adjustment results (analysis of residuals)

Simultaneous:
- Compensation by network arrangement
- Self-calibration by additional parameters

In the following only the method of self-calibration will be addressed because it has proved to be the most flexible and powerful technique, while requiring at the same time no additional measurement effort.

Self-calibration by additional parameters essentially consists in expanding the right hand side of (2) by additional functions which are supposed to model the systematic image errors according to

$$\begin{aligned} x_{ij} &= -c_j f_{ij}^x + x_{0j} + \Delta x_{ij}\,, \\ y_{ij} &= -c_j f_{ij}^y + y_{0j} + \Delta y_{ij}\,. \end{aligned} \tag{7}$$

The terms $\Delta x_{ij}, \Delta y_{ij}$ can be understood as corrections to the image coordinates x_{ij}, y_{ij} in order to reduce the physical reality of the sensor geometry to the perspective model. Obviously the principal point coordinates x_{0j}, y_{0j} can be considered part of this correction term. If a parameter for the camera constant is added, the full interior orientation is included in the additional parameter set.

The formulation of the additional parameter function is very crucial for a successful self-calibration. The actual physically caused deformations, which are a priori unknown in structure and magnitude, should be modelled as closely and as completely as possible. On the other hand, the chosen parameter set must be safely determinable in a given network arrangement. These are essentially two conflicting aspects which will be addressed in Section 3.3.2.4.

In aerial photogrammetry the sources for systematic errors have been studied in great detail and are generally quite well understood and modelled [9].

An international test has shown that different modelling concepts lead to practically the same results as long as the systematic errors are fully covered in the respective models [10].

In photographic close-range systems the following functions have proved to be effective [11]:

$$\begin{aligned}\Delta x &= -\Delta x_0 + \frac{\bar{x}}{c}\Delta c + \bar{x}s_x + \bar{y}a + \bar{x}r^2k_1 + \bar{x}r^4k_2 + \bar{x}r^6k_3 + \left(r^2 + 2\bar{x}^2\right)p_1 + 2\bar{x}\bar{y}p_2\,,\\ \Delta y &= -\Delta y_0 + \frac{\bar{y}}{c}\Delta c \;+\; 0 \;+\; \bar{x}a + \bar{y}r^2k_1 + \bar{y}r^4k_2 + \bar{y}r^6k_3 + 2\bar{x}\bar{y}p_1 + \left(r^2 + 2\bar{y}^2\right)p_2\,,\end{aligned} \tag{8}$$

$$with\ \bar{x} = x - x_0, \qquad \bar{y} = y - y_0, \qquad r^2 = \bar{x}^2 + \bar{y}^2$$

(the indices $_{ij}$ are left out here for the sake of simplicity)

This is called a "physical model", because all its components can directly be attributed to physical error sources. The individual parameters represent:

$\Delta x_0, \Delta y_0, \Delta c \ldots$	Change in interior orientation elements
s_x	Scale factor in x ("affinity")
a	Shear factor (jointly in x, y)
$k_1, k_2, k_3,$	First three parameters of radial symmetric lens distortion (k_3 is a priori disregarded if normal- and wide-angle lenses are used)
p_1, p_2	First two parameters of decentering distortion

Equations (8) has also proved to be successful in CCD-camera systems [2, 3] and will be used in the investigations of this paper.

The location of the principal point is not specified for most CCD-cameras, varies from camera to camera and depends on the configuration of the frame grabber. The scale factor in x is required to model the imprecise specification of the sensor element spacing and additonal imprecisions introduced with PLL line-synchronization. In the latter case the pixel spacing in x must be computed from the sensor element spacing, the sensor clock frequency and the sampling frequency with:

$$psx = ssx\frac{f_{sensor}}{f_{sampling}} \tag{9}$$

with

psx	Pixel spacing in x
ssx	Sensor element spacing in x
f_{sensor}	Sensor clock frequency
$f_{sampling}$	Sampling frequency of frame grabber

The shear factor a must be included to compensate for the geometric deformation which can be induced by PLL line-synchronization [3]. The use of additional parameters leads to an extended bundle model

$$\boldsymbol{l} - \boldsymbol{e} = \boldsymbol{A}\boldsymbol{x} + \boldsymbol{A_3}\boldsymbol{z}. \tag{10}$$

$\boldsymbol{z}, \boldsymbol{A_3}$ ..... Vector of additional parameters and associated design matrix

In a general bundle concept all unknown parameters are treated as stochastic variables. This permits to consider a priori information about these parameters to be included and includes both extreme cases where parameters are either excluded from the model or may be treated as free unknowns. If we split the vector $\boldsymbol{x}$ into its components $\boldsymbol{x_p}$ (for object point coordinates) and $\boldsymbol{t}$ (for exterior orientation parameters) we obtain the following estimation model:

$$\begin{array}{rcccccccl}
-\boldsymbol{e_B} & = & \boldsymbol{A_1 x_p} & + & \boldsymbol{A_2 t} & + & \boldsymbol{A_3 z} & - & \boldsymbol{l_B} \;;\; \boldsymbol{P_B} \\
-\boldsymbol{e_p} & = & \boldsymbol{I\, x_p} & & & & & - & \boldsymbol{l_p} \;;\; \boldsymbol{P_p} \\
-\boldsymbol{e_t} & = & & & \boldsymbol{I\, t} & & & - & \boldsymbol{l_t} \;;\; \boldsymbol{P_t} \\
-\boldsymbol{e_z} & = & & & & & \boldsymbol{I\, z} & - & \boldsymbol{l_z} \;;\; \boldsymbol{P_z}
\end{array} \tag{11}$$

$\boldsymbol{e_B}, \boldsymbol{e_p}, \boldsymbol{e_t}, \boldsymbol{e_z}$	Vectors of true errors of image coordinates, object point coordinates, exterior orientation elements, additional parameters
$\boldsymbol{l_B}, \boldsymbol{l_p}, \boldsymbol{l_t}, \boldsymbol{l_z}$	Vectors of observations of image coordinates (minus constant term from Taylor expansion), object point coordinates, exterior orientation elements, additional parameters
$\boldsymbol{P_B}, \boldsymbol{P_p}, \boldsymbol{P_t}, \boldsymbol{P_z}$ ...	Associated weight coefficient matrices
$\boldsymbol{x_p}, \boldsymbol{t}, \boldsymbol{z}$, ...	Parameter vectors of object point coordinates, exterior orientation elements, additional parameters
$\boldsymbol{A_1}, \boldsymbol{A_2}, \boldsymbol{A_3}$	Associated design matrices
$\boldsymbol{I}$	Identity matrix

In the investigations of Section 3.3.3 we will treat all control point coordinates with infinite weight (diag $(\boldsymbol{P}_p) \rightarrow \infty$), that is error-free and with $\boldsymbol{l}_p = \boldsymbol{0}$ (which leads to $\boldsymbol{x_p} = \boldsymbol{0}$, as $\boldsymbol{x_p}$ does not represent the full coordinate values but because of previous linearization only the incremental corrections). All other object points will be considered as "new points" with $\boldsymbol{P}_p = \boldsymbol{0}$ and $\boldsymbol{l}_p = \boldsymbol{0}$. The same will apply to all exterior orientatiom elements: $\boldsymbol{P}_t = \boldsymbol{0}$, $\boldsymbol{l}_t = \boldsymbol{0}$. In some cases the additional parameters will also be assumed as free unknowns, with $\boldsymbol{P}_z = \boldsymbol{0}$,

$\boldsymbol{l}_z = \mathbf{0}$. The stabilizing effect of finite (nonzero) weights for additional parameters in case of weak determinability was shown by *Gruen* [7], [9] and will also be addressed below.

3.3.2.4 Treatment of additional parameters

In (11) a unique set of additional parameters may be introduced for all participating frames or, as it is necessary if each frame comes from a different CCD-camera, an individual set may be assigned to each frame. Especially in the latter case the danger of overparameterization becomes apparent. This is the reason for the need to have a powerful parameter control procedure available, for the automatic detection of non-determinable parameters and their exclusion from the system.

In the past such procedures have been developed by different researchers. They all rely on statistical concepts. The procedures have never been compared to each other in an independent test. *Gruen* has published this approach in a series of papers [7, 9, 12, 13]. In the following a summary of this procedure will be given.

Conditions for the algebraic determinability of additional parameters were previously formulated by *Gruen* [7] and are reiterated in Appendix A. Since it is necessary in practice to deal with erroneous observations, the purely algebraic approach must be given up in favour of a statistical approach. Therefore any decisions will be correct only with a certain probability. The major problem consists in finding criteria for the rejection of individual parameters. The checking of parameters must be related to the purpose of the triangulation. Here three different objectives must be distinguished:

(a) Point position

(b) Optimum estimation of the elements of exterior orientation, e.g. for egomotion purposes

(c) Analysis of systematic image errors aimed at the optimum estimation of these errors

Objective (a) involves the optimum estimation of object space coordinates. Additional parameters are used as supporting variables for the improvement of the estimation model; they do not have a separate, independent meaning. Hence their statistical significance is not a matter of concern, unless insignificant parameters cause a substantial decrease of the redundancy in small systems. The precision measures of the object space coordinates are the system's only available meaningful parameters for quality control. In other words, those additional parameters that would cause an inadmissibly large deterioration of the network's precision measures have to be excluded. The most popular precision measures are the mean and maximal variance of the object point coordinates. It is necessary to check to what extent those measures are deteriorated by certain additional parameters. When designing a rejection procedure it is essential to keep in mind that the time requirements of many projects do not allow the use of computationally expensive methods for data analysis.

Since the determinability of additional parameters may vary largely, their checking should be done at different stages of the least squares adjustment process, using rejection criteria with varying sensitivity levels. The following stepwise procedure can be operated in a reasonably fast mode.

(1) In order to avoid a quasi column rank deficiency in the design matrix of the estimation model, the additional parameters are introduced as observed variables. The assignment of small weights assures that only a very small constraint is applied.

(2) Very poorly determined additional parameters can be deleted in the course of the factorisation procedure of the normal equations. Weakness of a particular additional parameter is indicated by a comparable small pivot element. If such a pivot falls short of a certain limit, the related additional parameter needs to be deleted. This can be achieved by adding a large number to this pivot element. The reduction process is continued.

(3) In a correlation check, high correlations indicate an inherent weakness of the system. They are particularly damaging if they occur between additional parameters and object point coordinates. Any additional parameter which leads to such correlations larger than 0.9 should be rejected. For computational reasons, only a few object points in characteristic locations may be included here.

(4) Detection and deletion are effected by those additional parameters that belong to the critical range between poorly determined and sufficiently well determined parameters. The trace check of the covariance matrix (outlined in Appendix B) may be used here.

(5) In a final step, the remaining additional parameters can be tested for significance, if this is considered necessary. It is suggested that the a posteriori orthogonalised additional parameter vector should be tested following the method outlined by *Gruen* [13]. The non-significant orthogonal components are set to zero. The back-transformation of the thus modified additional parameter vector from the orthogonal space to the "regular" space provides for a cleaned additional parameter set, involving the significant part only.

3.3.3 Determinability of self-calibration parameters under various network conditions

In the following we will show with the help of practical data to what extent individual or sets of additional parameters (APs) can be determined under varying network conditions. Our 3-D testfield is used as the object to be measured.

Figure 2 shows schematically the object and the arrangement of CCD-camera stations. For image acquisition a SONY- XC77CE camera with a 9 mm lens was used. The imagery was acquired with a VideoPix frame grabber using PLL line-synchronization. The resultant imagery has a size of 768 x 575 pixels. The sampling rate of the frame grabber was approximately 14 MHz, resulting in a pixel spacing of about $11\mu m$. A total of 36 object points were measured, 24 on the wall and 12 on the structure. Figure 3 shows a typical CCD image. The average number of measured image points per frame is 31.

The following parameters will be varied in our computational versions:

- Number of frames used in bundle adjustment (1, 2, 3, 4, 8).
- Configuration of frames (small base - parallel optical axes; large base - convergent optical axes; additional rotation of frames by 90^o at the approximate position of the non-rotated frames)

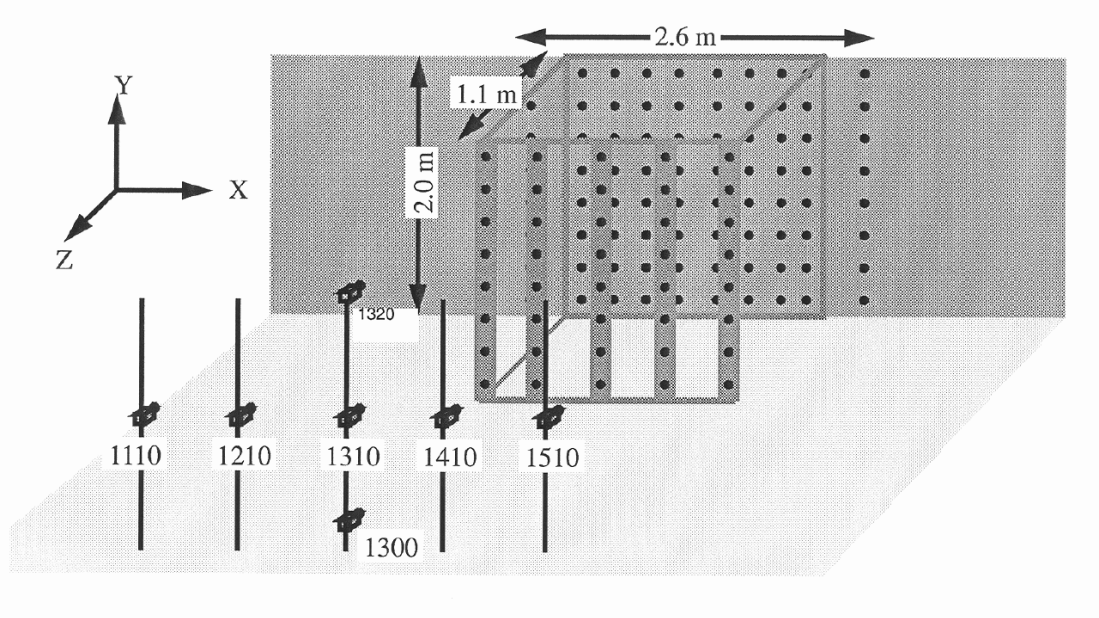

Figure 2: : Schematic perspective view of the test arrangement

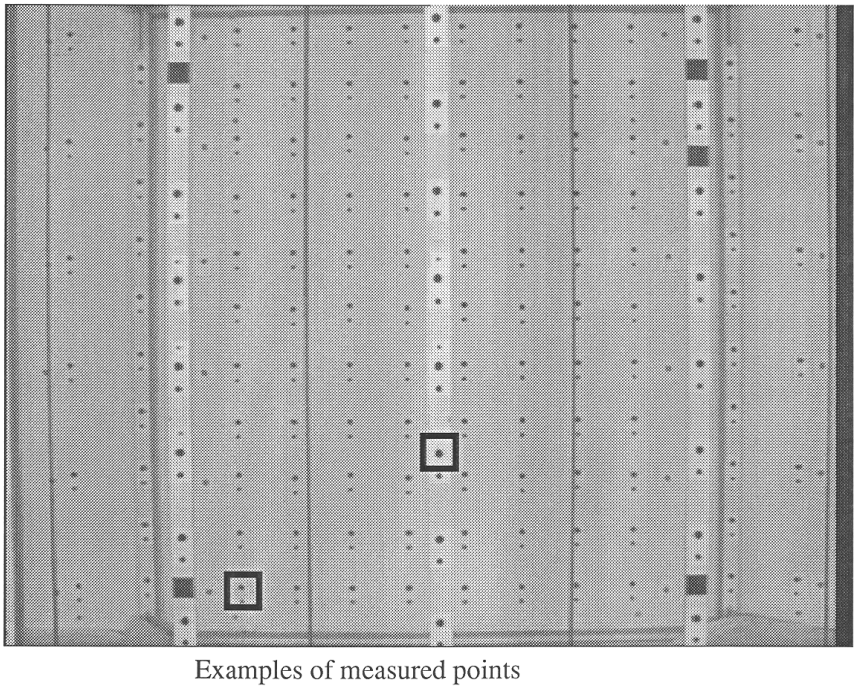

Figure 3: : Image grabbead at station 1310. The average number of measured points is 31 per image from a total of 36 object points.

Table 2: : Overview of versions. Image numbers with xxx1 denote that the camera was rotated by 90 degrees around its optical axis

Versions	Frames	Configuration	Images	APs
1xxxx	1		1310	Δx_H, Δy_H, Δc observed
21xxxx	2	1	1210, 1410	
22xxxx	2	2	1110, 1510	
3xxxx	3		1110, 1310, 1510	
41xxxx	4	1	1110, 1300, 1320, 1510	
42xxxx	4	2	1110, 1111, 1510, 1511	
81xxxx	8	1	1110, 1111, 1300, 1301, 1320, 1321, 1510, 1511	
82xxxx	8	2	1110, 1111, 1300, 1301, 1320, 1321, 1510, 1511	all free

- Object depth (plane object - rear wall, two depth planes - rear wall and three rods in the foreground)
- Number of object space control points (min, 3, 4, 5, 8, 9).“Min” stands for 7 control coordinates, the minimum number for all versions including more than one frame.
- Number of additional parameters $(0, 3\,[\Delta x_0, \Delta y_0, \Delta c]\,, 4, 5, 9)$. The full set of 9 APs is given by (8) leaving out k_3.

Table 2 shows together with Figure 2 the frame and configuration versions together with an indication as to how the APs are treated a priori (observed or free).

The results of computations are listed in Appendix C, Tables C1 to C7. Besides the estimated accuracy of the image coordinates ($\hat{\sigma}_0$) and the average standard deviations of the object points ($\bar{\sigma}_X, \bar{\sigma}_Y, \bar{\sigma}_Z$, or $\bar{\sigma}_{XYZ}$) the maximum correlations are listed (AP-OP: between APs and object point coordinates, AP-EO: between APs and exterior orientation elements, AP-AP: between APs only). The inherent correlation between k_1 and k_2 ($> 90\%$) is not included. The control point versions are selected according to the use of targets in one and two planes, i.e. for one plane: min, 3, 4, 5, 9 and for two planes: min, 4, 5, 8 control points. The control points have standard deviations of 0.0 (1.e-31) mm in X, Y, and Z. Standard deviation of a priori unit weight is 1.1 micrometer or 1/10th of the pixel spacing. The image coordinates have weight 1. $\Delta x_0, \Delta y_0, \Delta c$ have a standard deviation of 0.1 mm when they are treated as observed (in some cases, which are marked, one of 1.0 or 0.01). All additional parameters are treated as free unknowns for versions 82xxxx.

Figures 4 to 10 show the results of Tables C1 to C7 graphically. The average standard deviation of all object coordinates ($\bar{\sigma}_{XYZ}$) is plotted against the number of additional parameters (APs) in order to show the influence of the latter onto the former in a particular network version. The following symbols are used throughout these figures:

Two object planes

One object plane

M Number of control points; M stands for "minimum"

As a general result, with increasing number of frames, larger bases and convergent optical axes, more explicit 3-D object extension and increasing number of control points, we get an improvement in the determinability of APs. Since a detailed analysis would require much space, we will restrict our comments in the following to the most prominent points. The analysis will be based solely on the evaluation of $\bar{\sigma}_X, \bar{\sigma}_Y, \bar{\sigma}_Z$, or $\bar{\sigma}_{XYZ}$ respectively. Any other aspects, like the amount of correlation which a certain AP generates, are not considered.!l

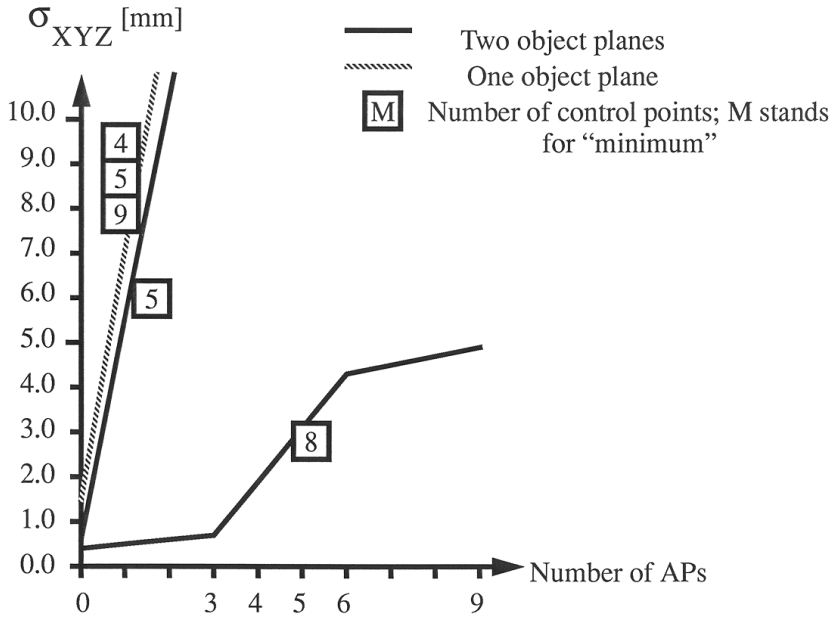

Figure 4: : One frame.

One frame (spatial resection): The elements of interior orientation cannot be determined as long as a plane object is used, independent of the number of control points. Other APs, however, might be determinable, given a sufficient number and distribution of control points. In the event of a substantial 3-D object extension the interior orientation is determinable, assuming at least five control points in appropriate 3-D distribution (here: three in one depth plane, two in the other). Attention: In version 12050, P=2, Co=5 only one control point has been used outside the rear plane, therefore all three interior orientation elements cannot be determined simultaneously (this one control point provides for only two image coordinate observations, whereas three parameters are to be determined).

Two frames (stereo, small base): Here some of the results look erratic. The versions with one object plane (P=1) produce partly better object point coordinate standard deviations if a larger a priori standard deviation for the interior orientation parameters is used (1 mm

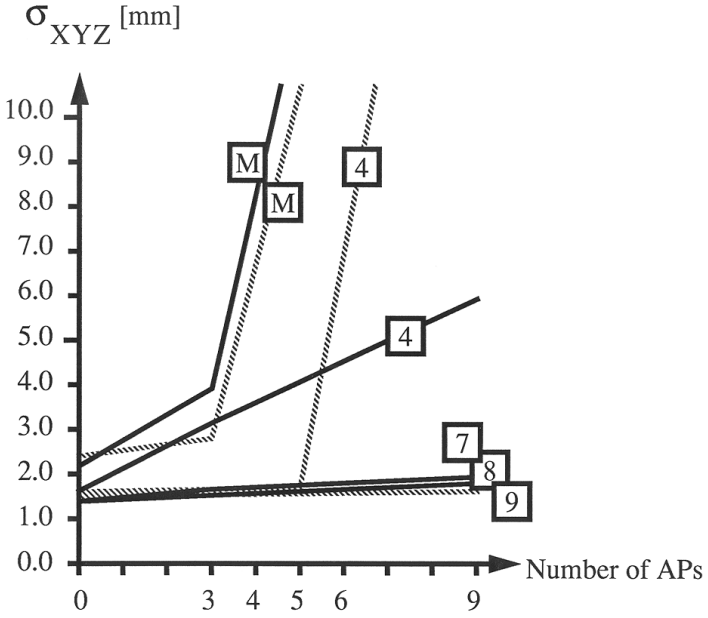

Figure 5: : Two frames, configuration 1.

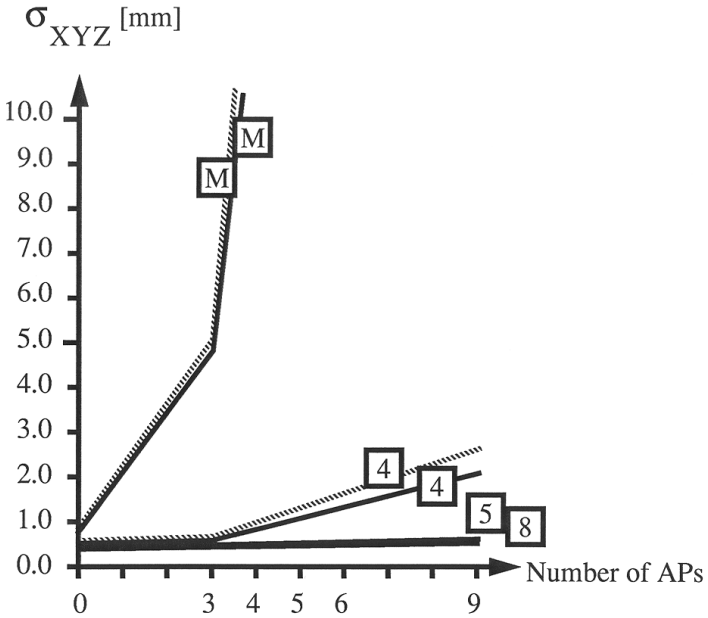

Figure 6: : Two frames, configuration 2.

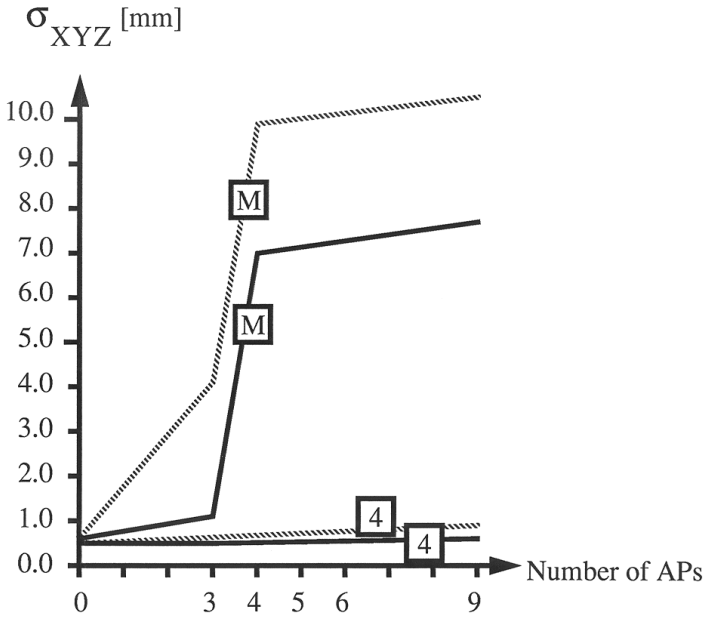

Figure 7: : Three frames

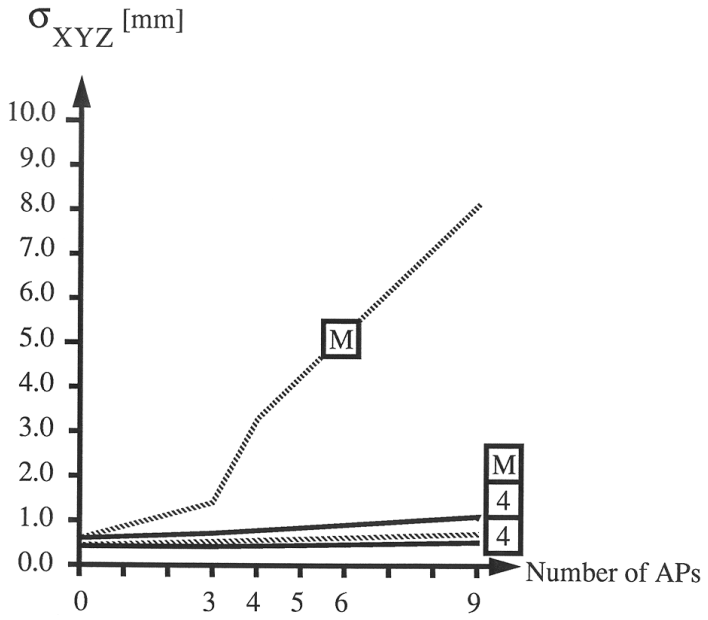

Figure 8: : Four frames, configuration 1.

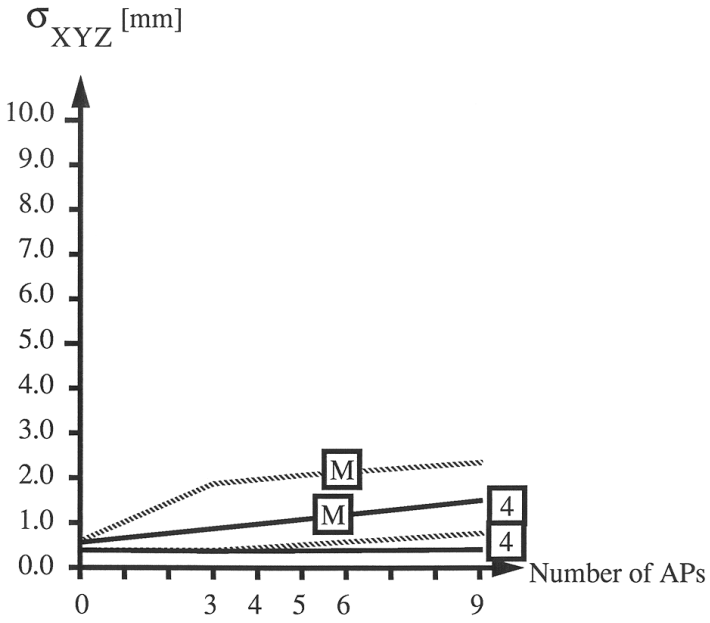

Figure 9: : Four frames, configuration 2.

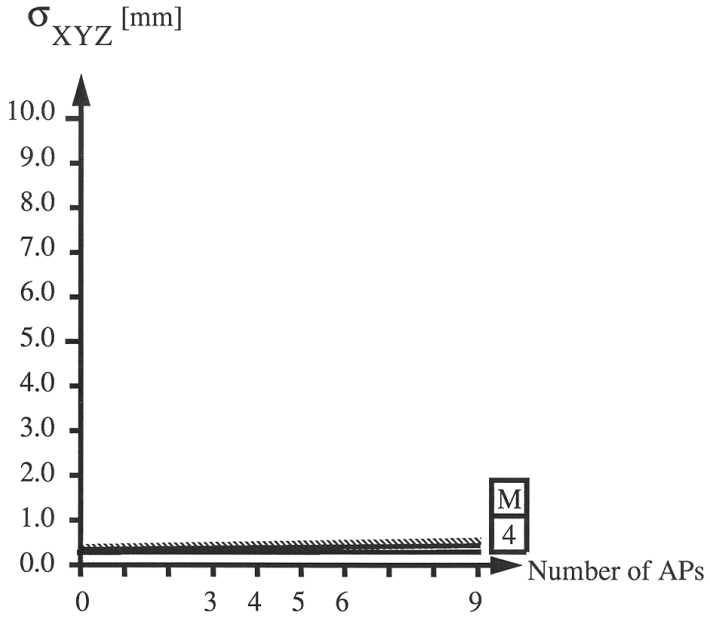

Figure 10: : Eight frames, configuration 1.

versus 0.1 mm). Also the values are partly too good to be possibly correct. This is due to the fact that all versions P=1, AP=3 are highly unstable (correlations AP-EO around 100%) so that any kind of numerical distortion may show up. It must be emphasized that in these computations the APs were not tested according to the procedure suggested in Sect. 3.3.2.4 and Appendix A, therefore highly instable APs were not automatically deleted prior to further analysis. Only with two object planes (P=2) and five control points (Co=5) or more we can get the interior orientation parameters (and other APs) accurately enough.

Two frames (convergent, large base): The previous situation changes in parts drastically if a larger base and convergent frames are used. Still in case of minimum control the principal point coordinates $\Delta x_0, \Delta y_0$ are not determinable, but this is corrected by an additional control point. For P=2 and five control points all nine APs are determined very well.

Three frames (large base plus center frame): As can be expected, this version gives better results than the previous version. While we still have problems with the minimum control versions, four control points give quite good results, especially in the two object planes (P=2) case.

Four frames (large horizontal base plus vertical base): Compared to the previous version we now obtain even in the case of minimum control / two planes good results for the interior orientation parameters and decent results for all nine APs. The corresponding one plane version is still weak in the interior orientation parameters and unacceptable for the other APs.

Four frames (large horizontal base plus additional 90% rotation of frames): As in the previous version, the four control point cases give good results up to all nine APs. However, the two plane/minimum control version is slightly worse, whereas the one plane / minimum control version gives substantially better results for nine APs than before, although it cannot be considered good enough yet.

Eight frames (large horizontal base plus vertical base plus additional 90% rotation of frames): Here we find excellent results in all versions, even for minimum control and only one object plane. Also, the use of a priori unconstrained APs does not worsen the results, as evidenced by the results of Table 3.

Summarizing the results, only the eight frames version was capable to produce very good results under all conditions assumed. Releasing either the nonredundant datum (minimum control) condition or the 3-D object condition even the four frames (two bases) arrangement may produce acceptable results. If only three frames are used, aligned along a common base, decent results can only be achieved with redundant control information ($\geq$ four control points). On the other hand, the results also show the inherent weakness of a two frames (stereo) system for self-calibration. It must be emphasized that these results have been obtained by using block-invariant additional parameters, that is one set of coefficients for all frames. If in robotics for example several CCD-cameras are utilized simultaneously and if problems, such as on-line focussing, zooming and compensation of damage caused by physical disturbances (vibrations, shocks, electrical distortions, etc.) have to be handled, a frame-invariant approach might be necessary and lead possibly to totally different conclusions than those presented here. In any case it would require a much more constrained environment. No matter what the actual approach is, a "blind" use of additional parameters is never recommended. In a concrete environment the geometrical conditions might be so complex

that it is very difficult to predict the results of self-calibration. Therefore the use of additional parameters should always be accompanied by a sophisticated checking and statistical testing procedure.

3.3.4 A final system test

This is to demonstrate the accuracy potential of CCD-camera based systems if the calibration is done properly.The version of 8 frames (large bases, convergent optical axes, 90 rotated frames, a priori unconstrained APs) was used with two control point versions (82200X: Minimum - seven coordinates, 82205X: Five full control points). The average standard deviation of image coordinates from least squares matching is 1.64 and 0.74 μm in x and y respectively. The targets are imaged on the average in 6.9 frames of the 8 frames used in the accuracy test. The image scale is 1 : 352. The targets are imaged on average with a diameter of 5.2 pixels, with a minimum of 3.5 and a maximum of 7.4. The average object distance is 3233 mm. The depth of the object is thus approximately 1/3 of the average object distance. Table 3 shows the results of computations.

The empirical RMSE (μ_X, μ_Y, μ_Z) agree well with the average standard deviations of the check point coordinates in the self-calibrating versions. The average accuracy improvement through self-calibration is around factor 12. Figure 11 shows the distribution of the check point residuals in the XY-plane. Globally this distribution looks rather random.

When analysing these results one should clearly keep in mind that the last measurement of the testfield's reference coordinates dates back 12 months and that at the time of comparison we had no indication of the quality of those coordinates. Figures 12, 13 and table 4 indicate the large effect of the radial symmetric distortion and the lesser influence of the other APs. At the corners of the CCD chip the radial symmetric distortion produces a displacement of 7.3 pixels. This large deformation is easily visible in the CCD frames (compare the bent rods in Figure 3). Table 4 gives the effect of the APs at a point with image coordinates $x = 3$ mm, $y = 2$ mm. It is evident that the major source of deformation is the radial symmetric distortion.

3.3.5 Conclusions

In the context of bundle adjustment the method of self-calibration presents a powerful tool for calibration and systematic error compensation in CCD-camera based vision systems. Moreover, it provides for accurate orientation and location of the sensor (spatial resection, egomotion) and for accurate reconstruction of the object space. As a prerequisite, however, the proper functions for modelling the systematic errors have to be chosen and a sophisticated checking and testing procedure for the additional parameters has to be incorporated. Furthermore, in order to provide for stable additional parameters and good determinability some geometrical conditions should be observed, like the use of more than two CCD frames with fairly large bases and convergent optical axes. Also, a 3-D object is to be preferred over a 2-D distribution of object points. These geometrical conditions may conflict with the requirements for successful image matching and image tracking in sequences (small disparities, "smooth" object, no occlusions, etc.), but a compromise should be aspired for.

Table 3: : Results of bundle adjustment. A priori standard deviations for additional parameters are infinity ($\hat{\sigma}_X, \hat{\sigma}_Y, \hat{\sigma}_Z$ were computed with $\sigma_0 = 1.1\mu m$)

Version	AP	Co	Ch	r	$\hat{\sigma}_0$ [µm]	$\bar{\sigma}_X$ [mm]	$\bar{\sigma}_Y$ [mm]	$\bar{\sigma}_Z$ [mm]	μ_X [mm]	μ_Y [mm]	μ_Z [mm]	μ_x [µm]	μ_y [µm]
822000	0	min	33	351	7.94	0.359	0.443	0.574	4.404	4.161	3.849	12.43	12.08
822009	9	min	33	342	1.53	0.382	0.462	0.574	0.338	0.325	0.529	1.09	1.05
822050	0	5	31	359	8.44	0.200	0.199	0.425	4.147	3.906	5.501	12.57	12.20
822059	9	5	31	350	1.52	0.221	0.225	0.427	0.306	0.314	0.503	1.05	1.02
Improvement 822000 / 822009					*5.2*	*0.94*	*0.96*	*1.0*	*13.0*	*12.8*	*11.4*	*11.4*	*11.5*
Improvement 822005 / 822059					*5.6*	*0.90*	*0.88*	*1.0*	*13.6*	*12.4*	*10.9*	*12.0*	*12.0*

AP..... Number of additional parameters
Co..... Number of control points
Ch ..... Number of check points
r ..... Redundancy
$\hat{\sigma}_0$..... Standard deviation of unit weight a posteriori; this corresponds to the estimated standard deviation of image coordinates
$\bar{\sigma}_X, \bar{\sigma}_Y, \bar{\sigma}_Z$.... Theoretical precision values of check point coordinates
μ_X, μ_Y, μ_Z ... Root Mean Square Errors from comparison of estimated coordinates to check point coordinates in object space
μ_x, μ_y ..... Root Mean Square Errors from comparison of estimated coordinates to check point coordinates in image space

Remark: The a priori weights of additional parameters are 0. For the computations of $\mu_X, \mu_Y, \mu_Z, \mu_x, \mu_y$ a 3-D similarity transformation onto all check points was performed before the comparison

As shown in this paper and in previous publications, even under relatively weak external constraints ($\leq$ five control points, eight CCD frames, standard set of block-invariant additional parameters, PLL line-synchronization) an accuracy of $1/10^{th}$ of a pixel or better for the X, Y-coordinates of well defined object points and a depth accuracy of 1/10 000 of the average object distance can be reached.

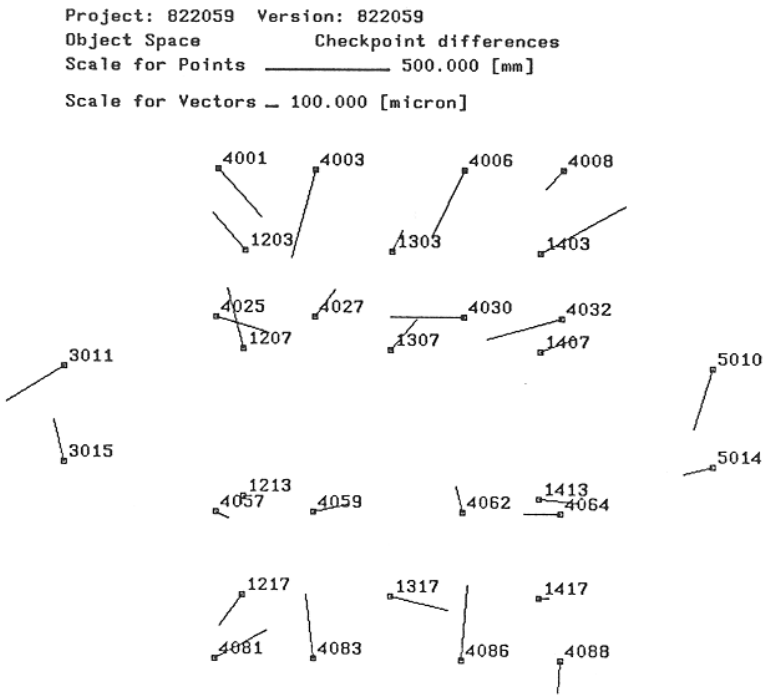

Figure 11: : Checkpoint residuals in XY-plane of object space (version 822059).

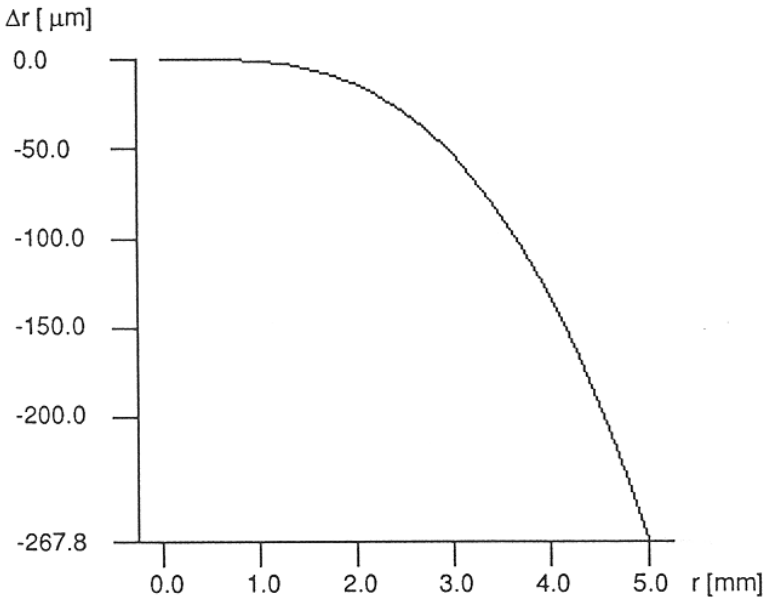

Figure 12: : Distortion profile using $k1$ and $k2$.

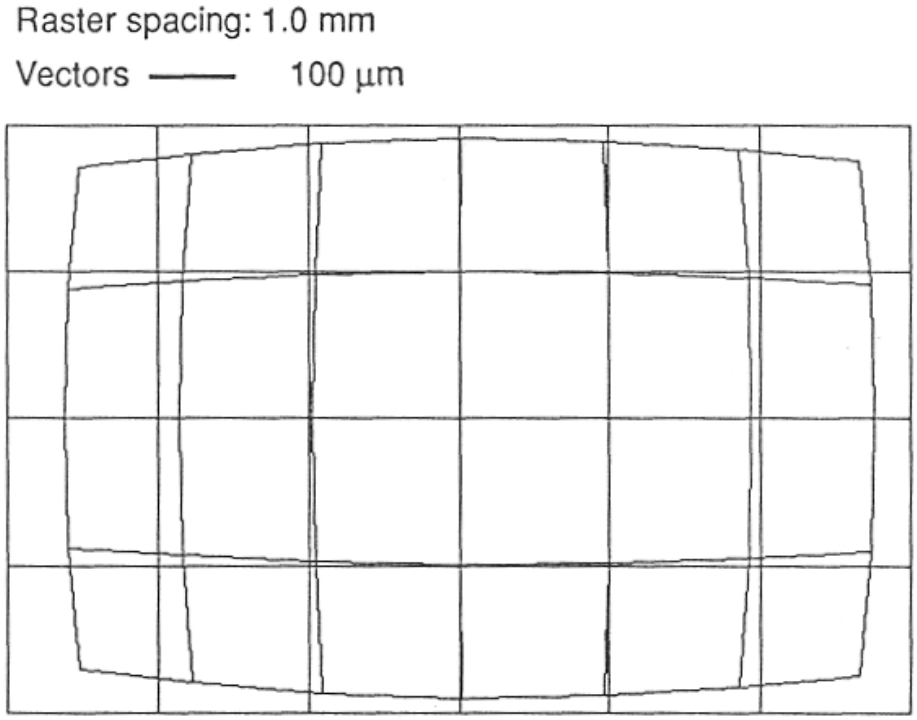

Figure 13: : Influence of additional parameters on grid.

Table 4: : Effect of additional parameters on point with image coordinates x=3, y = 2 mm

Parameter Number	Parameter	Influence in x	Influence in y
		[µm]	[µm]
4	Scale in x	0.02	0.00
5	Shear	-0.00	-0.01
6	k1	-81.47	-58.18
7	k2	16.52	11.80
9	p1	1.10	0.45
10	p2	-0.26	0.47

Appendix A
Algebraic determinability of additional parameters

An observation vector $\boldsymbol{l_{RS}}$ may include random and systematic components, i.e. a true random error $\boldsymbol{e_R}$ and a true systematic error $\boldsymbol{e_S}$.Then we obtain

$$\boldsymbol{e_R} + \boldsymbol{e_S} = \boldsymbol{l_{RS}} - E(\boldsymbol{l_R}) = \boldsymbol{l_{RS}} - \boldsymbol{Ax}\,, \tag{A1}$$

and the estimators for $\boldsymbol{x}$ and/or σ_0^2

$$\begin{aligned} \bar{\boldsymbol{x}} &= \left(\boldsymbol{A^T P A}\right)^{-1} \boldsymbol{A^T P l_{RS}}\,, \\ \bar{\sigma}_0^2 &= \frac{\boldsymbol{v_{RS}^T P v_{RS}}}{r} \end{aligned} \tag{A2}$$

are no more unbiased, if the systematic errors are not modeled and determinable by additional parameters.

We get the residuals $\boldsymbol{v_{RS}}$ to

$$\boldsymbol{v}_{RS} = -\left(\boldsymbol{I} - \boldsymbol{A}\left(\boldsymbol{A^T P A}\right)^{-1} \boldsymbol{A^T P}\right) \boldsymbol{l}_{RS}\,, \tag{A3}$$

$$\begin{aligned} \boldsymbol{v}_{RS} &= -\left(\boldsymbol{I} - \boldsymbol{A}\left(\boldsymbol{A}^T\boldsymbol{P}\boldsymbol{A}\right)^{-1} \boldsymbol{A}^T\boldsymbol{P}\right)(\boldsymbol{e_R} + \boldsymbol{e_S}) = \\ &= -(\boldsymbol{I} - \boldsymbol{K})(\boldsymbol{e_R} + \boldsymbol{e_S}) = \boldsymbol{M e_R} + \boldsymbol{M e_S}\,. \end{aligned}$$

$\boldsymbol{v_{RS}}$ is but a visible component of the random and the systematic errors.
The systematic component

$$\boldsymbol{v_S} = \boldsymbol{M e_S}\,, \tag{A4}$$

plays an important role in determination problems of systematic errors.
A systematic error is undeterminable, if

$$\boldsymbol{v}_S = \boldsymbol{M e}_S = (\boldsymbol{K} - \boldsymbol{I})\,\boldsymbol{e}_S = \boldsymbol{0}\,. \tag{A5}$$

In this case even additional parameters cannot provide for a determination.
Proof: Let $\boldsymbol{A}_1\boldsymbol{x}_1 = \boldsymbol{l} - \boldsymbol{e}_S$; $\boldsymbol{P}$ be the linear system for the estimation of $\boldsymbol{x}_1$ and $\boldsymbol{e}_S$ the true systematic error vector.
For the residual vector $\boldsymbol{v_S}$ we obtain

$$\boldsymbol{v}_S = -\left(\boldsymbol{I} - \boldsymbol{A}_1\left(\boldsymbol{A}_1^T\boldsymbol{P}\boldsymbol{A}_1\right)^{-1} \boldsymbol{A}_1^T\boldsymbol{P}\right)\boldsymbol{e}_S = \boldsymbol{M e}_S\,.$$

Let $\boldsymbol{A}_1\boldsymbol{x}_1 + \boldsymbol{A}_2\boldsymbol{x}_2 = \boldsymbol{l} - \boldsymbol{e}_S$; $\boldsymbol{P}$ be the same linear system, extended by the additional parameter function $\boldsymbol{A}_2\boldsymbol{x}_2$ which describes the systematic error $\boldsymbol{e}_S$.

Then the corresponding normal equations result in

$$\begin{pmatrix} \boldsymbol{A}_1^T\boldsymbol{P}\boldsymbol{A}_1 & \boldsymbol{A}_1^T\boldsymbol{P}\boldsymbol{A}_2 \\ \boldsymbol{A}_2^T\boldsymbol{P}\boldsymbol{A}_1 & \boldsymbol{A}_2^T\boldsymbol{P}\boldsymbol{A}_2 \end{pmatrix} \begin{pmatrix} \hat{\boldsymbol{x}}_1 \\ \hat{\boldsymbol{x}}_2 \end{pmatrix} = \begin{pmatrix} \boldsymbol{A}_1^T\boldsymbol{P}\boldsymbol{l} \\ \boldsymbol{A}_2^T\boldsymbol{P}\boldsymbol{l} \end{pmatrix},$$

and for the estimator $\hat{\boldsymbol{x}}_2$ we obtain

$$\begin{aligned} \boldsymbol{L}\hat{\boldsymbol{x}}_2 &= \left(\boldsymbol{A}_2^T\boldsymbol{P}\boldsymbol{A}_2 - \boldsymbol{A}_2^T\boldsymbol{P}\boldsymbol{A}_1\left(\boldsymbol{A}_1^T\boldsymbol{P}\boldsymbol{A}_1\right)^{-1}\boldsymbol{A}_1^T\boldsymbol{P}\boldsymbol{A}_2\right)\hat{\boldsymbol{x}}_2 = \\ &= \boldsymbol{A}_2^T\boldsymbol{P}\left(\boldsymbol{I} - \boldsymbol{A}_1\left(\boldsymbol{A}_1^T\boldsymbol{P}\boldsymbol{A}_1\right)^{-1}\boldsymbol{A}_1^T\boldsymbol{P}\right)\boldsymbol{l} = -\boldsymbol{A}_2^T\boldsymbol{P}\boldsymbol{v}_S\,. \end{aligned}$$

If $\boldsymbol{v}_S = \boldsymbol{0}$ we get the homogeneous linear system $\boldsymbol{L}\hat{\boldsymbol{x}}_2 = \boldsymbol{0}$. The non-trivial solutions $\hat{\boldsymbol{x}}_2 \neq \boldsymbol{0}$ are only existent if $\boldsymbol{L}$ is singular, what however implies the impossibility to obtain a unique solution $\hat{\boldsymbol{x}}_2 \neq \boldsymbol{0}$ for $\boldsymbol{x}_2$.

A reformulation of (A5) yields

$$\boldsymbol{M}\boldsymbol{e}_S = (\boldsymbol{K} - \lambda I)\ \boldsymbol{e}_S = \boldsymbol{0},\ \text{with}\,\lambda = 1\,. \tag{A6}$$

Because $\boldsymbol{M}$ is singular, $\det(\boldsymbol{M}) = 0$ is always valid, so that other solutions than $\boldsymbol{e}_S = \boldsymbol{0}$ are existent. The solution vectors for $\boldsymbol{e}_S$ can be interpreted as the eigenvectors for the eigenvalue $\lambda = 1$ of $\boldsymbol{K}$. The existency of $\lambda = 1$ follows from the idempotency of $\boldsymbol{K}$ and the rank deficiency $d_K \neq n$.

There may even exist more than one linear independent eigenvectors ; their number is u ($u = d_M$ = rank deficit of $\boldsymbol{M}$ = rank($\boldsymbol{K}$), if $\boldsymbol{P}$ is regular), because u-fold eigenvalues $\lambda = 1$ are possible.

All that means that for every bundle system u independent vectors of systematic errors exist, which are not determinable. It becomes an interesting and essential question, whether this mathematical set of errors includes some vectors which are physically possible, and moreover, which do occasionally or even often appear in practical projects.

In [7] an example of two types of systematic errors, which are often met in practical projects, is given. In [9] the previous concept has been extended to include gross errors (blunders) as well, and has also been supported by examples.

Appendix B
Trace check of covariance matrix

This procedure represents a computationally efficient technique to compute the effect of an individual additional parameter (or a group) on the trace of the covariance matrix of the other parameters of a bundle system, or a subset therefrom. It is based on the matrix identities

$$\tilde{\boldsymbol{N}} = \boldsymbol{N} + \boldsymbol{U}\boldsymbol{W}\boldsymbol{V}\,, \tag{B1}$$

$$\tilde{\boldsymbol{N}}^{-1} = \boldsymbol{N}^{-1} - \boldsymbol{N}^{-1}\boldsymbol{U}\left(\boldsymbol{W}^{-1} + \boldsymbol{V}\boldsymbol{N}^{-1}\boldsymbol{U}\right)^{-1}\boldsymbol{V}\boldsymbol{N}^{-1}\,. \tag{B2}$$

Assume that a self-calibrating bundle system with a full set of additional parameters generates the normal equation matrix $\boldsymbol{N}$ and the related weight coefficient matrix $\boldsymbol{Q_{xx}}$.
The deletion of one or more additional parameters leads to the normal equation matrix $\tilde{\boldsymbol{N}}$ and to $\tilde{\boldsymbol{Q}}_{xx}$ respectively.
In order to delete the additional parameter of column (i) of $\boldsymbol{N}$, a sufficiently large number is to be added to the diagonal element n_{ii} of $\boldsymbol{N}$. In the context of (B1), the addition of a large number w_{ii} may be represented as

$$\tilde{\boldsymbol{N}} = \boldsymbol{N} + \boldsymbol{u}_i w_{ii} \boldsymbol{v}_i^T \tag{B3}$$

with

$$\boldsymbol{u}_i^T = \boldsymbol{v}_i^T = 0, \ldots., 1, \ldots., 0\,;$$
$$(1, \ldots, (i), \ldots, u)\,.$$

Thus w_{ii} may be interpreted as a weight of an a priori observed additional parameter. If the observation is assumed to be 0, a large weight causes the parameter (i) to be forced to this observed value 0. For $\tilde{\boldsymbol{N}}^{-1}$ we obtain

$$\tilde{\boldsymbol{N}}^{-1} = \boldsymbol{N}^{-1} - \boldsymbol{N}^{-1}\boldsymbol{u}_i\left(\frac{1}{w_{ii}} + \boldsymbol{v}_i^T\boldsymbol{N}^{-1}\boldsymbol{u}_i\right)^{-1}\boldsymbol{v}_i^T\boldsymbol{N}^{-1}, \tag{B4a}$$

or

$$\tilde{\boldsymbol{Q}}_{xx} = \boldsymbol{Q}_{xx} - \boldsymbol{Q}_{xx}\boldsymbol{S}\boldsymbol{Q}_{xx}\,. \tag{B4b}$$

The matrix $\boldsymbol{S}$ given by

$$\boldsymbol{S} = \boldsymbol{u}_i\left(\frac{1}{w_{ii}} + \boldsymbol{v}_i^T\boldsymbol{Q}_{xx}\boldsymbol{u}_i\right)^{-1}\boldsymbol{v}_i^T \tag{B5a}$$

has the particular simple structure

$$\boldsymbol{S} = \begin{bmatrix} 0 & . & . & . & 0 \\ . & . & & & . \\ . & . & s_{ii} & . & . \\ . & & & . & . \\ 0 & . & . & . & 0 \end{bmatrix} \tag{B5b}$$

with

$$s_{ii} = \frac{1}{1/w_{ii} + q_{ii}} \,. \tag{B6a}$$

q_{ii} is the ith diagonal element of $\boldsymbol{Q}_{xx}$ and for $w_{ii} \to \infty$,

$$s_{ii} = \frac{1}{q_{ii}} \,. \tag{B6b}$$

Applying the trace operator tr to (B4b), we obtain

$$tr\left(\tilde{\boldsymbol{Q}}_{xx}\right) = tr\left(\boldsymbol{Q}_{xx}\right) - tr\left(\boldsymbol{Q_{xx}} \boldsymbol{S} \boldsymbol{Q_{xx}}\right) . \tag{B7}$$

With (B5b) and (B6b), the trace correction term $\Delta tr = tr\left(\boldsymbol{Q_{xx}} \boldsymbol{S} \boldsymbol{Q_{xx}}\right)$ takes the particular simple form

$$\Delta tr = tr\left(\boldsymbol{Q_{xx}} \boldsymbol{S} \boldsymbol{Q_{xx}}\right) = \frac{1}{q_{ii}} \sum_{j=1}^{u} q_{ij}^2 \,, \tag{B8}$$

where u is the number of system parameters in $\boldsymbol{N}$.
Hence, in order to check the influence of one additional parameter (i) on the trace of the covariance matrix, we need to compute only the ith row/column of $\boldsymbol{N}^{-1}$. If $\boldsymbol{N}$ is once factorised, the computational amount for that is not more than $O(A,\, M) = u^2 - 2u + 1$ (where $O(A,\, M)$ represents the number of additions and multiplications).
An equivalent expression to (B8) for the deletion of a set of addition parameters can readily be derived along the same lines.
Introducing the correlation coefficient ρ_{ij}, where

$$\rho_{ij}^2 = \frac{q_{ij}^2}{q_{ii}\; q_{jj}} \,, \tag{B9}$$

equation (B8) becomes

$$\Delta tr = tr\left(\boldsymbol{Q_{xx}} \boldsymbol{S} \boldsymbol{Q_{xx}}\right) = \sum_{j=1}^{u} \rho_{ij}^2 q_{jj} \,. \tag{B10}$$

Instead of checking the complete trace, it might be even more conclusive only to check the subtrace that is related to the object point coordinates. With u_i as the number of object point coordinates and $\boldsymbol{Q_{xx}^{ui}}$ the weight coefficient submatrix for object point coordinates, we would obtain

$$\Delta tr = tr\left(\boldsymbol{Q_{xx}^{ui}} \boldsymbol{S} \boldsymbol{Q_{xx}^{ui}}\right) = \frac{1}{q_{ii}} \sum_{j=1}^{u_1} q_{ij}^2 = \sum_{j=1}^{u_1} \rho_{ij}^2 q_{jj} \,; \qquad i \neq j \tag{B11}$$

Hence we get the alteration of the mean variance $\Delta\sigma_M^2$ of a network's point coordinates caused by one particular additional parameter (i) to

$$\Delta\sigma_M^2 = \sigma_0^2 \frac{1}{u_i} \sum_{j=1}^{u_i} \rho_{ij}^2 q_{jj} \,. \tag{B12}$$

Equation (B12) can be interpreted as a modified weighted mean, whereby the squared correlation coefficients ρ_{ij}^2 serve as "weighting factors" for the weight coefficients q_{jj} of the object point coordinates.
Individual variances may be checked by

$$\Delta q_{jj} = q_{jj} - \tilde{q}_{jj} = \rho_{ij}^2 q_{jj}\,, \tag{B13}$$

$$\begin{aligned} \tilde{\sigma}_{jj}^2 &= \sigma_0^2 \left(1 - \rho_{ij}^2\right) q_{jj}\,, \\ \Delta\sigma_{jj}^2 &= \sigma_0^2 \rho_{ij}^2 q_{jj}\,. \end{aligned} \tag{B14}$$

Appendix C
Results of computational versions for the determinability of additional parameters

V	Version number
F	Number of frames
C	Configuration of images for given number of frames
P	Number of target planes
Co	Number of control points
Ch	Number of check points
$\hat{\sigma_0}$	Standard deviation of unit weight a posteriori
$\bar{\sigma}_X, \bar{\sigma}_Y, \bar{\sigma}_Z$	Mean standard deviations of check point coordinates
$\sigma_{X_0}, \sigma_{Y_0}, \sigma_{Z_0}$ ...	Standard deviations of perspective center coordinates

Table C1: One frame

V	F	P	Co	Ch	AP	$\hat{\sigma}_0$ [µm]	σ_{X_0} [mm]	σ_{Y_0} [mm]	σ_{Z_0} [mm]	Max. Correlation in % AP-OP	AP-EO	AP-AP
11030	1	1	3	0	0	n.a.	2.75	2.59	0.57			
11040	1	1	4	0	0	2.21	1.94	1.83	0.40			
					3	2.03	33.80	33.77	36.65	0.0	100.0	0.1
11050	1	1	5	0	0	17.5	1.65	1.73	0.40			
					3	17.5	32.26	32.24	36.48	0.0	100.0	0.3
					5	24.1	36.30	36.31	36.44	0.0	100.0	45.9
11090		1	9	0	0	21.7	1.36	1.55	0.32			
					3	21.6	30.94	30.92	36.16	0.0	100.0	1.6
					9	2.02	35.54	35.67	35.44	0.0	99.5	52.5
12050	1	2	5	0	0	12.8	0.64	0.72	0.40			
					3	1.75	1.03	6.25	35.96	0.0	100.0	92.5
12080	1	2	8	0	0	31.8	0.43	0.50	0.24			
					3	1.99	0.53	0.50	1.04	0.0	97.7	2.2
					6	0.87	0.55	0.70	7.39	0.0	99.6	99.8
					9	0.93	2.22	2.47	7.65	0.0	100.0	99.9

Table C2: Two frames, configuration 1. Note: Versions marked with "1" have been computed using standard deviations of 1.0 mm for $\Delta x_H, \Delta y_H, \Delta c$

V	F	C	P	Co	Ch	AP	$\hat{\sigma}_0$ [µm]	$\bar{\sigma}_X$ [mm]	$\bar{\sigma}_Y$ [mm]	$\bar{\sigma}_Z$ [mm]	Max. Correlation in % AP-OP	AP-EO	AP-AP	Note
211000	2	1	1	min	21	0	9.36	0.942	1.475	3.747				
						3	9.36	1.320	2.519	3.749	87.6	99.4	0.0	
						3	9.15	49.96	48.87	2.59	95.5	93.1	26.7	1
211040	2	1	1	4	20	0	9.67	0.648	0.618	2.748				
						3	8.99	0.697	0.637	2.809	54.8	100.0	3.1	
						3	8.74	0.478	0.432	1.898	95.1	100.0	17.9	1
						5	8.97	0.715	0.653	2.845	53.9	100.0	26.2	
211090	2	1	1	9	15	0	10.2	0.569	0.568	2.484				
						3	9.98	0.593	0.574	2.514	38.3	100.0	5.9	
						3	9.88	0.293	0.279	0.744	88.4	100.0	22.9	1
						9	6.11	0.626	0.633	2.770	45.6	94.1	92.4	
212000	2	1	2	min	33	0	8.66	1.102	1.798	3.219				
						3	8.62	1.835	4.269	4.928	97.6	99.6	8.3	
						3	8.60	12.853	33.032	26.929	99.8	99.7	84.1	1
212040	2	1	2	4	32	0	9.06	0.722	0.704	2.698				
						3	8.62	1.835	2.194	4.646	98.7	100.0	9.5	
						9	6.21	5.358	5.091	7.242	98.7	99.5	81.8	
212050	2	1	2	5	31	0	10.8	0.555	0.552	2.281				
						3	9.19	0.756	0.804	2.715	95.2	99.9	71.0	
						9	6.29	0.744	0.777	3.173	64.5	90.6	83.6	
212080	2	1	2	8	28	0	13.6	0.529	0.519	2.295				
						9	6.28	0.638	0.651	2.977	60.6	98.2	89.6	

Table C3: Two frames, configuration 2

V	F	C	P	Co	Ch	AP	$\hat{\sigma}_0$ [µm]	$\bar{\sigma}_X$ [mm]	$\bar{\sigma}_Y$ [mm]	$\bar{\sigma}_Z$ [mm]	Max. Correlation in % AP-OP	AP-EO	AP-AP
221000	2	2	1	min	21	0	7.68	0.693	0.612	1.092			
						3	7.68	5.542	6.862	1.094	99.4	99.9	0.0
221040	2	2	1	4	20	0	7.9	0.424	0.401	0.813			
						3	1.24	0.461	0.432	0.851	44.2	95.7	11.5
						9	0.99	3.243	3.025	1.109	97.0	99.8	98.4
222000	2	2	2	min	33	0	12.5	0.694	0.700	0.912			
						3	12.5	4.963	6.614	1.689	99.8	100.0	30.2
						4	12.7	69.531	11.263	33.075	100.0	98.8	88.5
222040	2	2	2	4	32	0	12.2	0.445	0.465	0.738			
						3	11.6	0.469	0.486	0.746	49.7	96.4	6.8
						9	1.05	2.03	1.510	2.660	99.3	99.7	99.5
222050	2	2	2	5	31	0	12.4	0.406	0.267	0.649			
						9	1.06	0.546	0.505	0.749	76.3	96.8	95.3
222080	2	2	2	8	28	0	15.8	0.376	0.343	0.632			
						9	1.4	0.473	0.412	0.688	63.3	98.5	95.2

Table C4: Three frames

V	F	P	Co	Ch	AP	$\hat{\sigma}_0$ [µm]	$\bar{\sigma}_X$ [mm]	$\bar{\sigma}_Y$ [mm]	$\bar{\sigma}_Z$ [mm]	Max. Correlation in % AP-OP	AP-EO	AP-AP
31000	3	1	min	21	0	3.09	0.496	0.536	0.924			
					3	3.08	3.376	6.306	1.017	99.5	99.9	80.8
					4	3.10	15.911	6.333	1.019	99.6	99.8	98.3
					9	1.26	16.286	8.144	1.035	99.1	99.7	97.8
31040	3	1	4	20	0	3.24	0.332	0.328	0.773			
					9	1.30	1.098	0.829	0.803	94.6	99.6	98.8
32000	3	2	min	33	0	11.5	0.514	0.644	0.823			
					3	9.12	0.860	1.713	0.880	97.7	99.4	42.3
					4	9.15	11.324	2.014	3.912	99.4	99.9	99.6
					9	1.22	12.308	2.868	4.288	99.9	99.8	99.5
32040	3	2	4	32	0	11.3	0.355	0.381	0.680			
					3	9.42	0.360	0.391	0.682	38.8	99.1	6.80
					9	1.29	0.794	0.466	0.758	94.4	99.5	99.1

Table C5: Four frames, configuration 1

V	F	C	P	Co	Ch	AP	$\hat{\sigma}_0$ [µm]	$\bar{\sigma}_X$ [mm]	$\bar{\sigma}_Y$ [mm]	$\bar{\sigma}_Z$ [mm]	Max. Correlation in % AP-OP	AP-EO	AP-AP
411000	4	1	1	min	21	0	3.36	0.437	0.486	0.879			
						3	3.29	1.104	2.038	0.901	98.4	99.6	47.5
						4	3.31	5.210	2.217	0.960	99.4	99.6	96.3
						9	1.64	10.466	9.644	0.944	99.1	99.7	98.9
411040	4	1	1	4	20	0	3.39	0.294	0.289	0.726			
						3	3.36	0.309	0.298	0.756	35.1	98.6	8.2
						9	1.67	0.708	0.701	0.740	88.8	99.5	98.7
412000	4	1	2	min	33	0	9.71	0.454	0.591	0.767			
						3	8.89	0.571	0.914	0.800	89.2	97.2	13.1
						9	1.57	1.234	1.150	0.918	90.7	96.8	84.2
412040	4	1	2	4	32	0	9.61	0.320	0.335	0.633			
						9	1.60	0.446	0.410	0.653	78.0	97.6	96.0

Table C6: Four frames, configuration 2

V	F	C	P	Co	Ch	AP	$\hat{\sigma}_0$ [µm]	$\bar{\sigma}_X$ [mm]	$\bar{\sigma}_Y$ [mm]	$\bar{\sigma}_Z$ [mm]	Max. Correlation in % AP-OP	AP-EO	AP-AP	Note
811000	8	1	1	min	21	0	3.18	0.348	0.370	0.652				
						9	1.52	0.475	0.486	0.658	77.7	87.2	83.9	1
						9	1.57	0.503	0.502	0.654	77.5	90.9	89.7	
811040	8	1	1	4	20	0	3.16	0.225	0.223	0.534				
						9	1.52	0.340	0.333	0.541	78.5	93.1	88.5	1
						9	1.57	0.355	0.347	0.538	79.1	95.0	92.3	
812000	8	1	2	min	33	0	7.94	0.356	0.448	0.579				
						9	1.49	0.375	0.464	0.581	33.7	87.5	90.8	1
						9	1.52	0.382	0.463	0.575	33.9	89.9	92.1	
812040	8	1	2	4	32	0	7.92	0.242	0.262	0.476				
						9	1.49	0.262	0.284	0.481	35.2	92.2	90.4	1
						9	1.52	0.265	0.287	0.478	35.0	93.5	93.4	

Table C7: Eight frames, configuration 1. Note: Versions marked with "1" have been computed using standard deviations of 0.01 mm for $\Delta x_H, \Delta y_H, \Delta c$

V	F	C	P	Co	Ch	AP	$\hat{\sigma}_0$ [µm]	$\bar{\sigma}_X$ [mm]	$\bar{\sigma}_Y$ [mm]	$\bar{\sigma}_Z$ [mm]	Max. Correlation in % AP-OP	AP-EO	AP-AP
421000	4	2	1	min	21	0	2.6	0.490	0.433	0.768			
						3	1.82	3.249	0.554	0.778	99.2	99.9	58.7
						5	1.68	3.543	0.564	0.770	99.4	99.9	64.0
						9	1.38	3.786	1.164	0.803	99.0	99.1	90.9
421040	4	2	1	4	20	0	2.59	0.300	0.283	0.573			
						3	2.09	0.307	0.299	0.596	42.1	94.6	7.2
						9	1.37	0.756	0.723	0.632	90.2	96.3	94.2
422000	4	2	2	min	33	0	6.86	0.500	0.500	0.663			
						9	1.36	2.225	0.968	0.941	98.7	99.6	90.3
422040	4	2	2	4	32	0	6.99	0.323	0.334	0.538			
						3	6.53	0.333	0.347	0.544	47.6	96.3	7.1
						9	1.39	0.365	0.379	0.557	46.7	96.2	94.3

References

[1] A. Gruen: Towards real -time photogrammetry. Photogrammetria, 42, pp. 209-244 (1988)

[2] H. Beyer: Some aspects of the geometric calibration of CCD-cameras. Proceedings ISPRS Intercommission Conference on "Fast Processing of Photogrammetric Data", Interlaken, Switzerland, June, 1987, pp. 68-81

[3] H. Beyer: Geometric and radiometric analysis of a CCD-camera based photogrammetric close-range system. Dissertation, No. 9701, ETH Zürich (1992)

[4] A. Gruen, H. Beyer: Real-time photogrammetry at the Digital Photogrammetric Station (DIPS) of ETH Zurich. Paper presented at the ISPRS Commission V Symposium, "Real-Time Photogrammetry - A New Challenge", June 16-19, Ottawa, and in: The Canadian Surveyor, Vol. 41., No. 2, Summer 1987, pp. 181-199 (1986)

[5] D.C. Brown 1958: A solution to the general problem of multiple station analytical stereotriangulation. RCA Data Reduction Technical Report, No. 43, Patrick Air Force Base, Florida (1958)

[6] D.C. Brown: Close-range camera calibration. Photogrammetric Engineering, 37 (8) (1971) pp. 855-866

[7] A. Gruen: Progress in photogrammetric point determination by compensation of systematic errors and detection of gross errors. Nachrichten aus dem Karten- und Vermessungswesen, Series II, 36, pp. 113-140 (1978)

[8] A. Gruen: Precision and reliability aspects in close-range photogramme. Phot. Journal of Finland, Vol.8, No. 2, pp.117-132 (1980)

[9] A. Gruen: Photogrammetric point positioning with bundle adjustment (in German). Institut für Geodäsie und Photogrammetrie, ETH Zürich, Mitteilungen Nr.40. (1986)

[10] E. Kilpelä: Compensation of systematic errors of image and model coordinates (Report of ISPRS WG III/3). Int. Arch. of Photogrammetry, Vol.23, B9, Hamburg (1980)

[11] D.C. Brown: The bundle adjustment - progress and prospects. Int. Arch. of Photogrammetry, Vol. 21, B3, Helsinki (1976)

[12] A. Gruen: Experiences with self-calibrating bundle adjustment. Presented Paper to the Convention of ACSM/ASP, Washington, D.C., March (1978)

[13] A. Gruen: Data processing methods for amateur photographs. Photogrammetric Record, 11 (65), pp. 567-579 (1985)